BIOCHEMISTRY
including biophysical chemistry & molecular biology
Article

Biochemistry **2009,** *48,* 7867–7877 7867
DOI: 10.1021/bi900146g

HIV-1 Peptide Vaccine Candidates: Selecting Constrained V3 Peptides with Highest Affinity to Antibody 447-52D†

Brenda Mester,[‡,||] Revital Manor,[‡,||] Amit Mor,[‡] Boris Arshava,[§] Osnat Rosen,[‡] Fa-Xiang Ding,[§] Fred Naider,[§] and Jacob Anglister*[,‡]

[‡]*Department of Structural Biology, Weizmann Institute of Science, Rehovot 76100, Israel, and* [§]*Department of Chemistry, College of Staten Island of the City University of New York, Staten Island, New York 10314* [||]*B.M. and R.M. contributed equally to the study*

Received January 29, 2009; Revised Manuscript Received June 24, 2009

ABSTRACT: The V3 region of the envelope glycoprotein gp120 of the human immunodeficiency virus type 1 (HIV-1) is a potential target for an anti-HIV-1 vaccine. Peptides corresponding to V3 form three variations of a β-hairpin conformation when bound to anti-V3 HIV-1 neutralizing antibodies. The conformation of a $V3_{IIIB}$ peptide bound to the 0.5β antibody, generated against an X4 gp120, has been postulated to represent the V3 conformation of X4 viruses while the conformations of a $V3_{MN}$ and a $V3_{CONSENSUS}$ peptide bound to the 447-52D human monoclonal antibody were postulated to represent the R5A and R5B V3 conformations of R5 viruses, respectively. To constrain the conformation of synthetic V3 peptides to these X4, R5A, and R5B conformations, we formed disulfide bonds between Cys residues whose location in a peptide template representing the entire $V3_{CONSENSUS}$ epitope recognized by the broadly neutralizing 447-52D antibody was changed systematically. In a previous study [Mor, A., et al. (2009) *Biochemistry 48*, 3288−3303] we showed that these constrained peptides adopted conformations resembling the three antibody-bound V3 conformations according to the location of the disulfide bonds. Here we show that these constrained peptides, with the exception of peptides in which the disulfide bond flanks the GPGR segment, retain high-affinity binding to the 447-52D antibody. Compared with peptides designed to mimic the X4 conformation, peptides designed to mimic either the R5A or R5B conformation had higher affinity to 447-52D. It is possible that constrained peptides which mimic the R5A and R5B conformations of the V3 and retain high-affinity binding to 447-52D are good candidates for eliciting a broad neutralizing antibody response similar to that of 447-52D.

The third variable region (V3)[1] of the envelope glycoprotein gp120 of the human immunodeficiency virus (HIV-1) was previously termed as the "principal neutralizing determinant" of HIV-1, since many HIV-1 neutralizing antibodies from infected individuals were found to be directed against it (*1*). The V3 sequence determines whether the virus will use the CCR5 or CXCR4 chemokine receptors as a coreceptor for gp120 binding (R5 and X4 viruses, respectively). Although the V3 is variable in its amino acid sequence, its structure is conserved, and it contains conserved sequence elements (*2*) that are probably required for coreceptor binding. Antibodies targeted against V3 prevent the binding of gp120 to CCR5 and CXCR4, thus blocking events leading to viral fusion (*3*, *4*). Accordingly, the V3 has been considered as one of the main targets for an anti-HIV-1 vaccine. However, in neutralization-resistant primary isolates the V3 is occluded and becomes exposed only after CD4 binding. As a result these viruses are not sensitive to neutralization by anti-V3 antibodies.

The antibody 447-52D (*5*) derived from an HIV-1 infected donor is one of the most potent and broadly neutralizing human monoclonal antibodies directed against V3. In a comprehensive study of HIV-1 broadly neutralizing antibodies, 447-52D neutralized 45% of the clade-B isolates tested and was capable of neutralizing both X4 and R5 viruses as well as many primary isolates (*6*, *7*). However, 447-52D failed to neutralize neutralization-resistant primary isolates in which the V3 is occluded (*7*). Recently, soluble CD4 was found to broaden the neutralization profile of this antibody as well as of other V3-directed monoclonal antibodies and vaccine sera against subtype B viruses (*8*, *9*). In principle, the occlusion of the V3 can be overcome by

†This study was supported by NIH Grants GM53329 (J.A.) and GM22087 (F.N.) and by the Horowitz Foundation, the Gurwin Foundation, and the Kimmelman Center. J.A. is the Dr. Joseph and Ruth Owades Professor of Chemistry, and F.N. is the Leonard and Esther Kurtz Term Professor at the College of Staten Island at the City University of New York.

*To whom correspondence should be addressed. E-mail: Jacob.Anglister@weizmann.ac.il. Phone: 972-8-9343394. Fax: 972-8-9344136.

[1]Abbreviations: $V3_{XXX}$, V3 of the xxx strain; $V3_{CONSENSUS}$, V3 with the consensus sequence of clade-B HIV-1 R5 viruses (this sequence is the same as $V3_{JR-FL}$ and $V3_{JR-CSF}$); $V3_{X###C-Y###C}$, constrained V3 peptide in which residues X and Y (at positions ###) were replaced by cysteines and a disulfide bond was formed between the cysteine residues; V3, the third variable loop of gp120; C4, the fourth constant region of gp120; HIV-1, human immunodeficiency virus type 1; SPR, surface plasmon resonance; Fab, antigen binding fragment of an antibody; k_{off}, dissociation rate constant; K_D, equilibrium dissociation constant.

Published on Web 06/24/2009

prophylactic administration of CD4-mimic compounds: either small organic molecules like NBD-556 (*10*), which can be given orally, or CD4-mimic peptides that can be given as microbicides (*11*). Administration of these compounds to V3-vaccinated individuals will expose the V3 of the infecting virus prior to its attachment to target cells, thus enabling neutralization by the vaccine-elicited antibodies. The broadening of the spectrum of HIV-1 isolates neutralized by V3-directed antibodies using CD4-mimic compounds would make a V3-based vaccine an attractive candidate for an anti-HIV-1 vaccine.

In principle, the entire envelope glycoprotein gp120 could be used as an anti-HIV-1 vaccine. However, this protein is a notoriously poor immunogen due to conformational masking (*12*), occlusion by carbohydrate (*13*), and the existence of immunosuppressor determinants (*14*). Monomeric gp120 contains many epitopes that are not exposed in the native trimeric structure of gp120 (*15*), thus diverting the immune response to non-neutralizing determinants. A stabilized trimeric gp140 which includes gp120 and the extracellular region of trans-membrane glycoprotein gp41 may lead to a poor anti-V3 antibody response because of V3 occlusion (*16*). The use of synthetic peptides as immunogens can focus the immune response on the neutralizing epitope and lead to a high level of neutralizing antibodies compared with the use of monomeric or trimeric gp120. Nevertheless, even constrained V3 peptides may contain epitopes that are irrelevant for neutralization.

Insights into the conformation of the V3 region presented to the immune system by HIV-1 should be useful for the design of an anti-HIV-1 vaccine. Therefore, we previously studied the structures of V3 peptides bound to the strain-specific HIV-1 neutralizing antibodies 0.5β and the broadly neutralizing antibody 447-52D (*17*). The structure of a $V3_{IIIB}$ peptide (V3 region of the HIV-1_{IIIB} strain) in complex with the 0.5β antibody Fv and the structure of three different V3 peptides corresponding to IIIB, MN, and JR-FL sequences in complex with 447-52D Fv were determined by NMR (*2*, *18*−*20*). All bound V3 structures showed a β-hairpin conformation. The X-ray structure of 447-52D Fab in complex with a $V3_{MN}$ peptide (*21*) was in excellent agreement with the NMR structure of an Fv-bound $V3_{MN}$ peptide (*18*). The structures of two additional anti-gp120 antibodies (2219 and F425-B4e8), directed against the V3, in complex with V3 peptides were solved recently by X-ray crystallography (*22*, *23*), and in both cases the bound V3 peptides formed a β-hairpin similar to that observed by NMR in Fv/V3−peptide complexes. Moreover, the structure of a V3-containing gp120 solved lately by Kwong and co-workers (*24*) exhibited an rmsd of 1.6 Å for the Cα atoms of residues 304−322 when compared with the previously published structure of a $V3_{CONSENSUS}$ peptide (the same sequence as $V3_{JR\text{-}FL}$ and $V3_{JR\text{-}CSF}$) bound to 447-42D (*25*). The excellent agreement among the NMR and the X-ray structures of the V3 suggests that the β-hairpin conformation represents the native conformation of the V3.

In all NMR and crystallographic studies of V3 peptides in complex with Fv or Fab fragments of different HIV-1 neutralizing antibodies, the N-terminal segment of the V3 and the reverse turn formed by the GPGR segment interacted extensively with the antibodies while the C-terminal segment exhibited considerably fewer interactions with the antibodies (*2*, *18*, *20*, *21*, *25*−*28*). As shown in Figure 1, two different variations of the N-terminal strand conformations have been observed: one that is recognized by the 0.5β antibody (*20*) and the other recognized by the 447-52D antibody (*2*, *18*, *25*). These two variations differ by a one

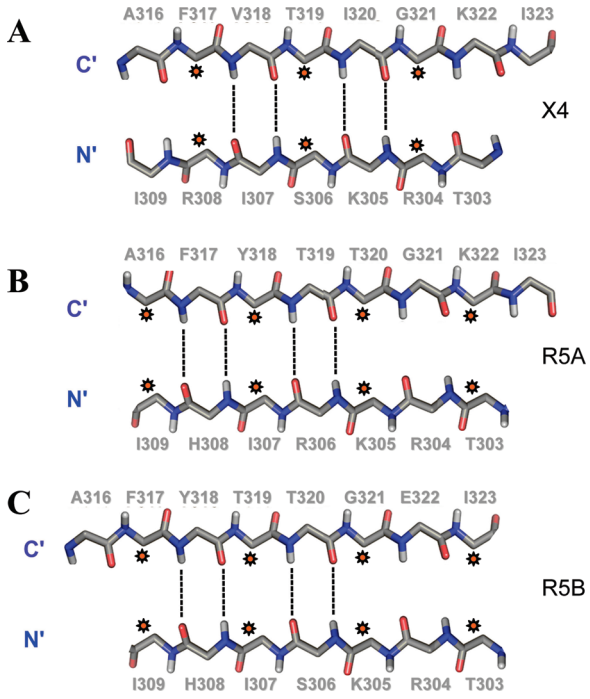

FIGURE 1: Residue pairing and hydrogen bond in the schematic structure of X4, R5A, and R5B of V3 (A, B, and C, respectively). The X4 structure is that of $V3_{IIIB}$ bound to 0.5β (*20*). The R5A and R5B structures are those of $V3_{MN}$ (*18*) and $V3_{CONSENSUS}$ (*25*), respectively, bound to 447-52D. Hydrogen bonds are indicated by dashed black lines. Possible locations for cysteine replacement for the disulfide bond are indicated by orange symbols.

register shift in the N-terminal strand residues that form hydrogen bonds within the β-hairpin (*18*). We postulated that the $V3_{IIIB}$ conformation bound to the 0.5β Fv represents the X4 conformation of the V3, while conformations of V3 peptides bound to 447-52D represent the R5 conformation (*18*). The conformations of $V3_{CONSENSUS}$ and $V3_{IIIB}$ bound to 447-52D differ from that of $V3_{MN}$ recognized by the same antibody in the pairing of the residues in the β-hairpin, resulting in a further differentiation to R5A ($V3_{MN}$) and R5B ($V3_{CONSENSUS}$, $V3_{IIIB}$) substructures (*2*, *25*). Since R5 and not X4 viruses are mostly involved in HIV-1 transmission (*8*), it is the R5 phenotype of HIV-1 that is most relevant for vaccine development, and we have been interested in constraining peptides to assume the postulated R5 conformations of the V3.

Synthetic peptides corresponding in sequence to the V3 region were previously suggested as a component of an anti-HIV-1 vaccine (*29*), and a few studies using HIV-1 and SHIV V3 peptides have demonstrated the induction of antibodies that neutralized homologous HIV-1 primary isolates (*30*−*34*). Recently, a linear 22-residue V3 segment (in the form of a C4-V3 peptide, where C4 stands for the fourth constant region of gp120), that resembles the consensus sequence of clade-B R5 viruses, was found to induce antibodies that neutralized 31% of the subtype B HIV-1 isolates that were evaluated (*29*). The antibody response to the C4 segment was rather limited (*35*), suggesting that immunization by C4-V3 peptides is a promising method to elicit broadly neutralizing anti-V3 antibodies provided that these antibodies can overcome the occlusion of the V3 observed in many HIV-1 primary isolates.

Linear V3 peptides are flexible in solution, and except for a turn formed by the conserved GPGR segment, they do not exhibit any well-defined structure (*36*, *37*). As a result, linear V3

peptides may elicit antibodies against numerous different structures, many of which do not resemble the native conformation of the V3. V3 peptides constrained by chemical means to adopt the native V3 conformation, i.e., the β-hairpin V3 conformation found by both NMR and crystallography, should be more efficient than linear V3 peptides in eliciting HIV-1 neutralizing antibodies. Although the constrained peptides may not adopt a conformation identical to that of native V3, they will assume a narrower conformational distribution in comparison to that formed by the unconstrained V3 peptide. Thus, a larger fraction of the antibodies elicited against the constrained peptide should recognize the V3 in the context of native gp120 on the infecting virus. Most importantly, in comparison with the predominantly unstructured linear V3 peptides, V3 peptides constrained to a β-hairpin conformation similar to that bound to 447-52D are more likely to elicit antibodies manifesting extensive backbone−backbone interactions between V3 and the CDRs of the antibody. This type of interaction, observed for the 447-52D complex with $V3_{MN}$, is probably one of the main reasons for the broad neutralization by this antibody.

Different methods, such as cyclization by disulfide bonds (*38*) and hydrazone-based cross-links (*39*, *40*), have been developed recently and used in attempts to constrain the conformation of V3 peptides (*39*, *41*, *42*). In most of these studies short V3 segments were used. For example, Cabezas and co-workers used a hydrazone link to constrain the segment HIGPGRAF to a β-hairpin conformation (*39*). This segment is eight residues shorter than the 447-52D epitope and ten residues shorter than the constrained V3 peptides used in this study. Moreover, unlike the peptides used in this study, the peptide used by Cabezas et al. (*39*) did not include residues K305 and I307, which form extensive interactions with 447-52D. Only one of the sera from the three rabbits immunized with an hydrazone-link constrained V3 peptide neutralized the laboratory-adapted strain $HIV\text{-}1_{MN}$, and neutralization of primary isolates was not tested (*39*).

As part of our program to develop a rational strategy to design peptide-based anti-HIV-1 vaccines, we previously studied the conformations of V3 peptides constrained by single and double disulfide bonds and by replacement of P313 by D-Pro (*43*). Our design of these peptides considered the register of the hydrogen bond-forming positions, especially in the N-terminal strand, and the pairing of the residues in the β-hairpin conformation. Proper placement of disulfide bonds was used to dictate specific pairing of opposing residues as well as the alignment of the hydrogen bond network between the two β-hairpin strands (*43*). Our NMR studies concluded that constraining the peptide by a single disulfide bond or D-Pro resulted in a conformation that partly resembled a β-hairpin in that the NOESY spectra of these analogues exhibited long-range side chain interactions between the N- and C-terminal strands of the V3. We have determined that a conformation similar to a β-hairpin conformation mimicking either the postulated X4 or the R5A conformation could be obtained using two disulfide bonds (*43*), thus demonstrating that the location of the disulfide bond can indeed dictate the hydrogen bond network in the constrained peptides.

In the present study we investigated the influence of the constraints on the affinity of the V3 peptides to the 447-52D antibody. Our results show that a single disulfide bond involving the replacement of either T303, or K305 or I307, with cysteine increased the affinity of the peptide to 447-52D. These peptides have the potential to elicit anti-V3 antibodies that will cross-react with HIV-1 although it is questionable whether antibodies that very closely resemble 447-52D in their neutralization potency can be elicited.

EXPERIMENTAL PROCEDURES

Peptide Synthesis. Peptide synthesis and purification as well as cyclization were discussed previously (*43*). All peptides used in the binding studies were greater than 95% pure as judged by HPLC and had the correct molecular mass.

Expression and Purification of 447-52D. IgG 447-52D (IgG3, λ) was prepared as described by Sharon et al. (*44*). Briefly, the monoclonal antibody 447-52D was purified from the supernatant of the hetero-hybridoma cells by affinity chromatography using a protein A column. The antibody was cleaved by papain as previously described (*44*). The cleavage reaction was stopped with iodoacetamide, and the Fab was then purified by size-exclusion chromatography using a Superdex 200 column. The Fab fraction was dissolved in sodium acetate buffer, pH 4.0, and was further purified on an SP-Sepharose cation-exchange column (GE Healthcare) using a gradient of NaCl with final concentration of 1 M.

Surface Plasmon Resonance (SPR) Measurements. Binding affinities (K_D) of Fab 447-52D to various biotinylated V3 peptides were determined by SPR using a Biacore3000 instrument (Biacore AB, Uppsala, Sweden) and a ProteOn XPR36 instrument (Bio-Rad Haifa, Haifa, Israel) (*45*). All experiments were carried out at 25 °C using standard HBS-EP buffer (0.01 M HEPES, pH 7.4, 0.15 M NaCl, 3 mM EDTA, 0.005% Surfactant P20). Peptides (100 ng/mL) were immobilized to a carboxymethylated dextran matrix chip, precoated with streptavidin (Biacore SA sensor chip, ProteOn NLC sensor chip). The immobilization procedure was allowed to continue until 30−50 RU (response units; 1 RU = 1 pg of protein/mm^2) of biotinylated V3 peptides were attached to the streptavidin-precoated surface of the chip. A blank reference sensor surface without an immobilized V3 peptide served as a negative control for the binding interaction. To test binding of Fab 447-52D to this surface, serial dilution of Fab 447-52D in a HBS-EP buffer (concentration ranging from nano- to micromolar, depending on the immobilized V3 peptide) was injected over the peptide-immobilized surface. All Fab injections were performed in duplicates or triplicates. The sensor surface was regenerated between each binding reaction by one wash with 50 mM aqueous NaOH for 60 s at flow rates of 20 and 30 μL/min (Biacore3000 and ProteOn XPR36, respectively). The regeneration step was followed by a blank injection in order to prevent analyte contamination by the regeneration reagent in the next binding reaction. Each binding curve was corrected for nonspecific binding by subtracting the signal obtained from the negative control channel. For binding experiments under reducing conditions, HBS-EP buffer with 2 mM DTT was used. The peptides were incubated overnight with 10 mM DTT, and the Fab injections were performed in HBS-EP buffer with 2 mM DTT. The injection method and data analysis scheme for each Fab concentration were adapted from Myszka (*46*).

Steady-State Binding Measurements. All steady-state binding measurements were performed using a Biacore3000 instrument (Biacore AB, Uppsala, Sweden). Association and dissociation phases were monitored for 600−750 and 200 s, respectively, at 20 μL/min flow rate. In cases where the injection time did not suffice to bring the reaction toward a complete steady-state regime (where $dRU/dt = 0$), the last 20 response

Table 1: Sequences and Kinetic Parameters of Single Disulfide Bond Constrained and Mutated Peptides[a]

(biotin+) Sequence	Peptide name	K_D (10^{-9} M)	k_{off} (10^{-3} sec^{-1})	K_{on} (10^6 $sec^{-1}M^{-1}$)	Constrained to
Clade-B consensus					
SGSTRKSIHIGPGRAFYTTGEI Under reduced conditions[c]	Linear-$V3_{CONSENSUS}$	0.84 ± 0.1 0.96 ± 0.1	0.43 ± 0.05 0.39 ± 0.05	0.51 ± 0.07 0.41 ± 0.06	
Single disulfide					
SGSTRKSIHCGPGRCFYTTGEI	V3(I309C-A316C)[b]	580 ± 50	121 ± 10	0.21 ± 0.02	R5A
SGSTRKSIHCGPGRACYTTGEI Under reduced conditions[c]	V3(I309C-F317C)	246 ± 26 2.7 ± 0.3	68 ± 4 2.19 ± 0.13	0.28 ± 0.02 0.81 ± 0.05	R5B
SGSTRKSICIGPGRACYTTGEI	V3(H308C-F317C)[b]	20 ± 2	9.5 ± 0.1	0.47 ± 0.05	X4
SGSTRKSCHIGPGRAFCTTGEI	V3(I307C-Y318C)	0.59 ± 0.04	0.39 ± 0.03	0.67 ± 0.02	R5A
SGSTRKSCHIGPGRAFYCTGEI	V3(I307C-T319C)	1.2 ± 0.2	0.28 ± 0.01	0.24 ± 0.01	R5B
SGSTRKCIHIGPGRAFYCTGEI	V3(S306C-T319C)	6.7 ± 0.1	2.4 ± 0.1	0.35 ± 0.06	X4
SGSTRCSIHIGPGRAFYTCGEI	V3(K305C-T320C)	0.17 ± 0.03	0.11 ± 0.03	0.65 ± 0.15	R5A
SGSTRCSIHIGPGRAFYTTCEI	V3(K305C-G321C)	0.36 ± 0.01	0.09 ± 0.03	0.25 ± 0.03	R5B
SGS_CKSIHIGPGRAFYTTC Under reduced conditions[c]	V3(R304C-G321C)	6.6 ± 0.2 9.0 ± 0.3	2.62 ± 0.05 2.89 ± 0.06	0.40 ± 0.01 0.32 ± 0.02	X4
SGSCRKSIHIGPGRAFYTTGC Under reduced conditions[c]	V3(T303C-E322C)	0.26 ± 0.06 1.1 ± 0.3	0.18 ± 0.01 0.48 ± 0.03	0.69 ± 0.04 0.44 ± 0.03	R5A
SGSCRKSIHIGPGRAFYTTGEC	V3(T303C-I323C)	0.52 ± 0.07	0.33 ± 0.07	0.63 ± 0.01	R5B
Alanine replacement					
SGSTRKSAHIGPGRAFYATGEI	V3(I307A)	11 ± 1	3.2 ± 0.2	0.29 ± 0.02	
SGSTRKSIHAGPGRAFYTTGEI	V3(I309A)[b]	24 ± 2	10.2 ± 0.3	0.42 ± 0.05	
SGSTRKSIHAGPGRSFYTTGEI	V3(I309A:A316S)	13 ± 3	3.9 ± 0.3	0.30 ± 0.01	
SGSTRKSIHAGPGRAAYTTGEI	V3(I309A:F317A)[b]	22 ± 2	11.0 ± 0.1	0.50 ± 0.04	
SGSTRKSIAIGPGRAAYTTGEI	V3(H308A:F317A)[b]	24 ± 2	11.5 ± 0.1	0.48 ± 0.03	
Penicillamine replacement					
SGSTRKSIHpGPGRpFYTTGEI	V3(I309p-A316p)[b]	2200 ± 300	122.0 ± 0.7	0.055 ± 0.005	R5A
SGSTRKSIHpGPGRApYTTGEI	V3(I309p-F317p)[b]	43 ± 3	3 ± 1	0.070 ± 0.08	R5B
SGSTRKSIpIGPGRApYTTGEI	V3(H308p-F317p)[b]	49 ± 4	8.6 ± 0.1	0.18 ± 0.02	X4
L-Pro313D-Pro					
SGSTRKSIHIG_{D}-PGRAFYTTGEI	V3(D-Pro)[b]	50 ± 2	27.9 ± 0.3	0.56 ± 0.02	
P313N					
SGSTRKSIHIGNGRAFYTTGEI	V3(P313N)[b]	No binding detectable			

[a] Error values in K_D represent the fitting error (errors in all other cases represent the SDs). Off-rates (k_{off}) were derived from data recorded at a slower than optimal flow of 20 μL/min. [b] Data were obtained by equilibrium experiment. [c] Data were obtained under reducing conditions; i.e., the peptides were incubated overnight with 10 mM DTT, and 2 mM DTT was added to the HBS-EP buffer containing 447-52D Fab.

signals were averaged and treated as the steady-state values. The dissociation rate constants (k_{off}) were obtained by globally fitting the dissociation phases of the experimental sensorgrams of each peptide to a single exponential equation with a locally fitted linear drift term. The steady-state SPR data points of the averaged duplicate or triplicate runs were plotted against the Fab concentration. To derive the steady-state binding constant (K_D), each of these plots was non-least-square fitted (NLSF) to a "one-site" binding model available in the Origin 7.0 package (OriginLab Corp.).

Kinetic Binding Measurements. V3 peptides with off-rates slower than 3 ms^{-1} were investigated using SPR kinetic measurements. Kinetic assays were performed using both a Biacore3000 instrument (Biacore AB, Uppsala, Sweden) and a ProteOn XPR36 instrument (Bio-Rad Haifa, Haifa, Israel). The unique feature of the ProteOn XPR36 system is its ability to collect binding data for six different analyte concentrations over six different target protein surfaces at one time (*45*). In kinetic assays, five or six Fab dilutions (nano- to micromolar concentration ranges) were injected over the peptide-immobilized surface at a flow rate of 75 μL/min for 250 s (Biacore3000) and 60 μL/min for 225 s (ProteOn XPR36) to monitor the association phase. The dissociation phase was subsequently measured by running the buffer over the peptide-immobilized surface at the same flow rate for a period of 1000 s. In cases where background or systematic noise reduction was necessary, kinetic data were "double referenced" by using a "blank" cycle, in which no Fab was present, in order to record the systematic noise of the system. The final sensorgrams were generated by subtracting both the signal of the negative control channel and the averaged response of the blank

injections from the entire data set (*46*). Kinetic parameters and binding affinities were obtained by globally fitting the data to a simple 1:1 Langmuir interaction model by using BIAevalution 3.1 software (Biacore AB, Uppsala, Sweden). Sensorgrams obtained by Biacore3000 were fitted by adding a local linear drift term.

Isothermal Titration Calorimetry (*ITC*). ITC measurements were carried on an iTC200 titration microcalorimeter (Microcal; GE Healthcare, NJ). The Fab and V3 peptides were dialyzed and dissolved, respectively, with HBS-EP buffer (same buffer that was used for SPR measurements). The sample cell (204 μL) was maintained at 25 °C and filled with a 3.6 μM Fab solution. The injection syringe was filled with either the linear (41 μM) or constrained (44 μM) peptide solutions. During the titration experiments, the sample solution was stirred at 1000 rpm with the injection syringe. After the establishment of a stable baseline, 0.4 μL of solution was injected to remove possible air bubbles at the syringe opening. Subsequently, a succession of 15 microinjections of 2.4 μL of the peptide solutions was made, with each injection separated by 2.5 min to allow the heat signal to return to the baseline. The isothermal titration curves were recorded and analyzed with ORIGIN software (Microcal Inc.), provided with the iTC200 instrument. A monovalent binding model was used to calculate the thermodynamic parameters. For high association constants ($K_a \geq 1\times10^8$ M^{-1}), only the enthalpy (ΔH) can be determined accurately from ITC measurements (*47*). Therefore, for calculating the entropy ($\Delta S°$), $\Delta G°$ was first calculated from the equation $\Delta G° = -RT \ln K_a$, where K_a is the reciprocal value of K_D that was obtained from SPR measurements, R is the ideal gas constant, and T is the absolute temperature. Subsequently, $\Delta S°$ was calculated by $\Delta S° = (\Delta H° - \Delta G°)/T$, where $\Delta H°$ is taken from the ITC experiment, $\Delta G°$ is taken from the calculation described above, and T is the absolute temperature.

RESULTS

Design of Peptides with a Single Disulfide Bond. The $V3_{IIIB}$ epitope recognized by the 0.5β antibody encompasses residues K305−I320 (16 residues), and the $V3_{MN}$ and $V3_{CONSENSUS}$ epitopes recognized by the 447-52D antibody include residues K305−T320 (14 residues) and R304−G321 (16 residues), respectively. The apparent disagreement between the epitope lengths of $V3_{MN}$ and $V3_{CONSENSUS}$ calculated on the basis of the numbering of the terminal residues and their actual lengths given in parentheses is due to the numbering of gp120 residues according to $gp120_{IIIB}$ which has a two-residue insertion, Q310-R311. In addition to residues 305−321, the structure of $V3_{CONSENSUS}$ bound to 447-52D included residue E322 which was found to form electrostatic interactions with R304 (*25*). This interaction may stabilize the β-hairpin conformation and dictate the pairing of the residues, and therefore, we have decided to include E322 in the peptides that we investigated. The sequence of the peptides we studied is based on the $V3_{CONSENSUS}$ sequence which represents the consensus sequence of clade-B R5 HIV-1 strains.

In the peptides constrained by a single disulfide bond, the location of the disulfide bond was changed systematically (see Table 1) in order to investigate its influence on the binding affinity of the constrained V3 peptides to 447-52D Fab. Initially, a disulfide bond was formed between cysteine residues replacing I309 and A316 which flank the conserved GPGR segment

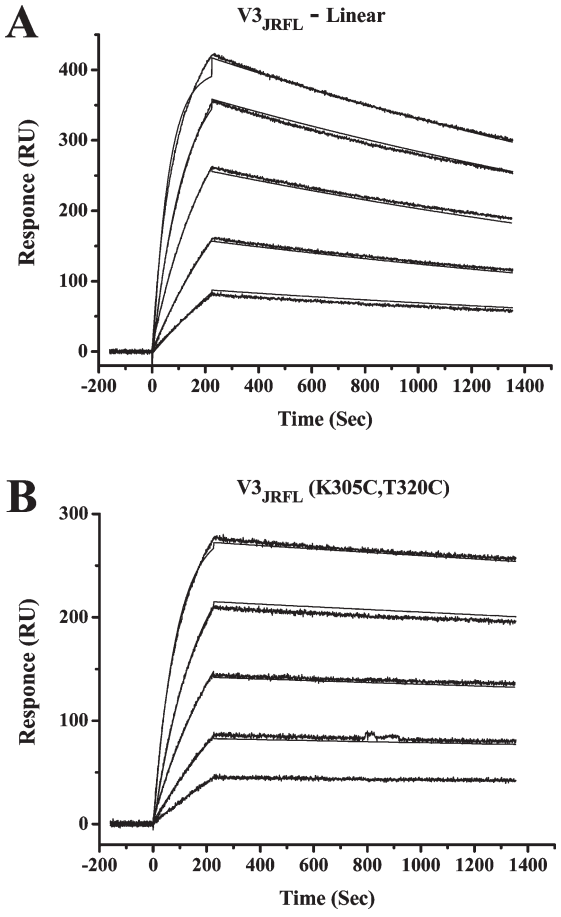

FIGURE 2: SPR binding measurements of two representative V3 peptides to Fab 447-52D. Kinetic sensorgrams of $V3_{CONSENSUS}$ linear (A) and $V3_{K305C-T320C}$ (B) peptides. Injection of Fab 447-52D at different concentrations (1.5625, 3.125, 6.25, 12, and 25 nM) was allowed for 225 s at a flow of 60 μL/min, while the dissociation phase was set for 1000 s for both peptides. Fitted curves (overlaid, represented by the thin black lines) were obtained using the 1:1 Langmuir binding model (ProteOn Manager Software 2 beta).

($V3_{I309C-A316C}$). Subsequently, the disulfide bond was moved systematically further away from the GPGR turn until T303 and I323 at the very ends of the epitope were replaced by cysteines ($V3_{T303C-I323C}$) in the last peptide. All peptides were preceded by a flexible linker (Ser-Gly-Ser) and were biotinylated at their N-termini.

Dissociation Constants and Off-Rates of Peptides Constrained by a Single Disulfide Bond. The binding of 447-52D Fab to the V3 peptides was measured by SPR using kinetic binding measurements (for V3 peptides with off-rates slower than 3 ms^{-1}) and/or steady-state equilibrium binding measurements as described in the Experimental Procedures. The kinetic on- and off-rates, k_{on} and k_{off}, respectively, were evaluated by analyzing the SPR sensorgrams. The dissociation constant, K_D, was then calculated from the kinetic constants ($K_D = k_{off}/k_{on}$). K_D values obtained for the constrained V3 peptides were compared to those obtained for the parent linear $V3_{CONSENSUS}$ peptide corresponding to residues 303−323 of $V3_{CONSENSUS}$ (biotin-SGSTRKSIHIGPGRAFYTTGEI). All peptides contained biotin-SGS at their N-terminus to facilitate the SPR measurements. Sensorgrams of the kinetic binding experiments for the linear $V3_{CONSENSUS}$ and $V3_{K305C-T320C}$ peptides (panels A and B of Figures 2, respectively) and a sensorgram of an equilibrium binding measurement for the peptide $V3_{I309C-A316C}$

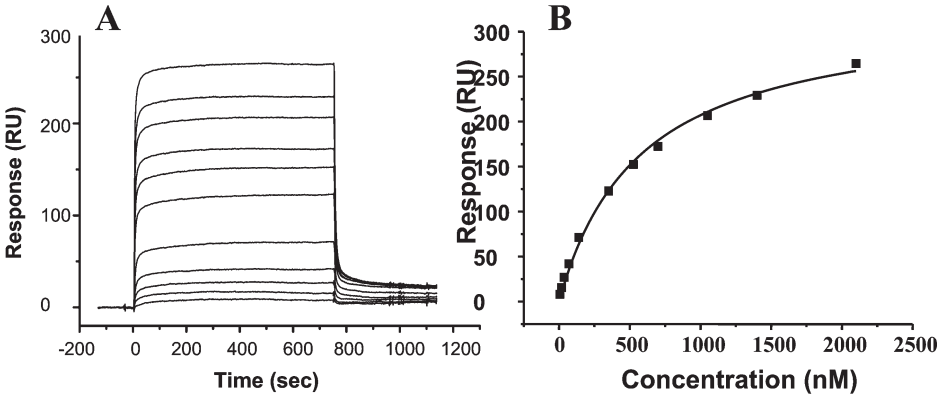

FIGURE 3: SPR binding measurements of $V3_{I309C-A316C}$ peptide to Fab 447-52D. Overlay plot of equilibrium sensorgrams for various concentrations (5.8, 17.5, 35, 70, 140, 350, 525, 700, 1050, 1400, and 2100 nM) (BIAevalution 3.1 software). Fab injection lasted for 750 s and was followed by a 200 s dissociation phase using a flow rate of 20 μL/min (A). The corresponding equilibrium binding curve: response (RU) as a function of Fab concentration is shown in (B). The black line represents the fit of the binding plot to a 1:1 binding model.

(Figure 3A) are representative of the quality of the data obtained. Figure 3B presents the titration plot constructed from the equilibrium experiment and its curve-fitted line. Table 1 summarizes the K_D, k_{off}, and k_{on} values determined for the linear and the constrained peptides.

The linear $V3_{CONSENSUS}$ peptide exhibited very tight binding with a dissociation constant of 0.84 ± 0.1 nM and an off-rate of 0.43×10^{-3} s^{-1}. This binding was weakened by more than 600-fold for the first constrained peptide $V3_{I309C-A316C}$ in which the disulfide bond flanks the conserved GPGR turn at the tip of the V3 β-hairpin and which was designed to mimic the R5A conformation of the V3 (*18*). In this peptide, I309 opposes A316 as in the structure of $V3_{MN}$ bound to the 447-52D Fv (*18*). When the size of the turn was increased from four to five residues to mimic the R5B conformation of the V3 (*25*), the dissociation constant of the peptide $V3_{I309C-F317C}$ increased by almost a factor of 300 in comparison with the linear $V3_{CONSENSUS}$ peptide. In this peptide, I309 opposes F317 as in the structure of $V3_{CONSENSUS}$ and $V3_{IIIB}$ bound to the 447-53D Fv (*25*). When the disulfide bond was placed further away from the GPGR segment, with six residues between the two cysteine residues ($V3_{H308C-F317C}$) the K_D increased only by 20-fold relative to the linear $V3_{CONSENSUS}$ peptide. A further increase in the distance of the disulfide bond from the GPGR segment resulted in additional improvement in the peptide binding affinity to 447-52D, and some of the peptides, most notably $V3_{I307C-Y318C}$, $V3_{K305C-T320C}$, $V3_{K305C-G321C}$, $V3_{T303C-E322C}$, and $V3_{T303C-I323C}$, which were designed to mimic either the R5A or the R5B conformation of the V3, bound more tightly to 447-52D than linear $V3_{CONSENSUS}$. However, the maximum improvement was only by up to 5-fold ($K_D = 0.17 \pm 0.03$ nM). Interestingly, in all peptides where Cys replacement was designed to mimic the X4 V3 conformation (see these positions in Figure 1 and Table 1), the dissociation constants were found to increase in comparison with peptides in which the disulfide bond involved one of the adjacent residues to mimic the R5 conformations of the V3 as illustrated in the diagram summarizing the dissociation constant data (Figure 4).

Dissociation Constants of Alanine Mutants. In order to isolate the influence of constraining the V3 peptide by a disulfide bond from the change in peptide binding due to amino acid replacement of $V3_{CONSENSUS}$ wild-type residues, five V3 peptides containing alanine replacements were synthesized, and their binding to 447-52D Fab was measured. K_D and k_{off} were

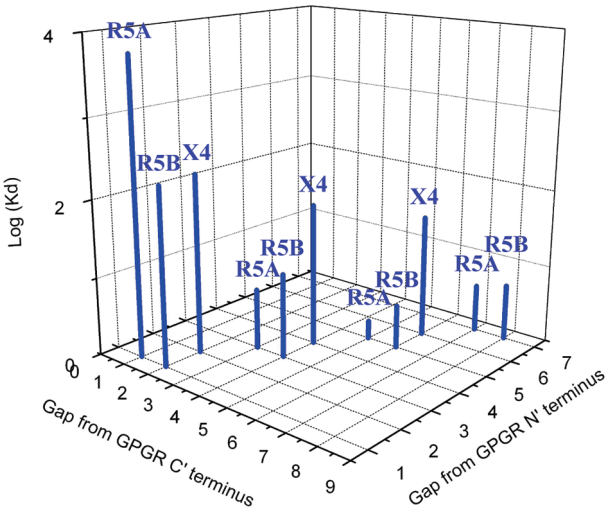

FIGURE 4: Dependence of the dissociation constants of 447-52D Fab complexes with constrained V3 peptides on the location of the disulfide as indicated by the number of residues (gap) between the cysteine residues at the N- and C-terminal strands and the GPGR segment. The postulated conformation is noted above the line.

evaluated as summarized in Table 1. Replacement of I307 or I309 resulted in approximately a 13- and 29-fold increase, respectively, in the dissociation constant relative to the K_D of the linear $V3_{CONSENSUS}$ peptide. Additional replacement of the C-terminal residues A316 (with serine) and F317 resulted in only minor changes in binding affinity as measured for the peptides $V3_{I309A-A316S}$ and $V3_{I309A-F317A}$, which had K_D of 13 and 22 nM, respectively. The considerable increases in the K_D of the modified peptides could be due to mutations in V3 residues interacting with the 447-52D antibody and/or due to changes in the propensity of the N- and C-strand residues to form a β-strand conformation.

Dissociation Constants and Off-Rates of Reduced Peptides. To further asses the influence of constraining the V3 peptide by a disulfide bond from the change in peptide binding due to cysteine replacement of consensus sequence V3 residues, the kinetic parameters of constrained versus reduced V3 peptides were compared. For this purpose, four peptides were selected: linear $V3_{CONSENSUS}$ and one representative from each conformation, R5A, R5B, and X4 ($V3_{T303C-E322C}$, $V3_{I309C-F317C}$ and $V3_{R304C-G321C}$, respectively), and their binding to 447-52D

Table 2: Sequences and Kinetic Parameters of V3 Peptides Constrained with Two Disulfide Bonds[a]

(biotin+) Sequence	Peptide name	K_D (10^{-9} M)	k_{off} (10^{-3} sec^{-1})	Constrained to
Clade-B consensus				
SGSTRKSIHIGPGRAFYTTGEI	Linear-$V3_{CONSENSUS}$	0.84 ± 0.1	0.43 ± 0.05	
Double disulfide				
SGSCRKSCHIGPGPAFCTTGCG	V3(T303C-E322C;I307C-Y318C)	0.78 ± 0.04	0.22 ± 0.01	R5A
SGSCRKSIHCGPGRCFYTTGCI	V3(T303C-E322C;I309C-A316C)	81 ± 9[b]	17 ± 1	R5A
SGSCRKSCHIGPGRAFYCTGEC	V3(T303C-I323C;I307C-T319C)	3.4 ± 0.1	0.92 ± 0.03	R5B
SGSTRCSIHCGPGRACYTTCEI	V3(K305C-G321C;I309C-F317C)	159 ± 5[b]	31 ± 4	R5B
SGSCRKSIHCGPGRACYTTGEC	V3(T303C-I323C;I309C-F317C)	108 ± 3[b]	38 ± 4	R5B
SGSGCKSICIGPGRACYTTCEI	V3(R304C-G321C;H308C-F317C)	280 ± 40[b]	7 ± 1	X4

[a] Error values in K_D represent the fitting error (errors in all other cases represent the SDs). Off-rates (k_{off}) were derived from data recorded at a slower than optimal flow of 20 μL/min. [b] Data were obtained by equilibrium experiment.

was measured in their oxidized (with disulfide bond) and reduced form (without disulfide bond). The $V3_{T303C-E322C}$ peptide, which exhibited 3-fold stronger binding compared with linear $V3_{CONSENSUS}$ displayed almost the same K_D under reducing conditions as the linear $V3_{CONSENSUS}$ peptide. The $V3_{I309C-F317C}$ peptide, which exhibited a 300-fold increase in K_D in comparison with linear $V3_{CONSENSUS}$, displayed only a 3-fold increase in K_D under reducing conditions. The 100-fold higher K_D observed for the oxidized constrained $V3_{I309C-F317C}$ peptide relative to the reduced unconstrained peptide likely reflects an unfavorable conformation induced by the disulfide bond when it is too close to the GPGR segment. The reducing conditions had almost no effect on the K_D of the $V3_{R304C-G321C}$ peptide which bound 447-52D 8−11-fold less strongly than linear $V3_{CONSENSUS}$. It is possible that the replacement of Arg304 by Cys eliminated the potential electrostatic interaction between Arg304 and Glu322 that could stabilize the β-hairpin conformation of the V3 (*25*). A disulfide bond between residues 304 and 321 does stabilize a β-hairpin but in the X4 V3 conformation and not in the R5 conformation recognized by 447-52D (*43*). The X4 conformation seems to have lower affinity to 447-52D in comparison with the R5A and R5B conformations (Table 1 and Figures 1 and 4). Thus, although the peptides with reduced and oxidized Cys at residues 304 and 322 both have lower affinity than linear $V3_{CONSENSUS}$ to 447-52D, these decreases likely result from different reasons.

Dissociation Constants of Penicillamine Analogues. Replacement of I307 and I309 with cysteine involves a change from a bulky hydrophobic residue containing a *sec*-butyl group ($CH(CH_3)(CH_2CH_3)$ in isoleucine) to a residue with much smaller hydrophobic surface (CH_2SH in cysteine). To examine whether substitution of two methyl groups in place of the methylene protons of cysteine could compensate for the loss of hydrophobic interactions, I307 and I309 were replaced with penicillamine ($C(CH_3)_2SH$) and oxidized to the corresponding disulfide bond. SPR measurements revealed that the $V3_{I309pen-A316pen}$ peptide exhibited an approximately 4-fold increase, $V3_{H308pen-F317pen}$ peptides exhibited approximately 2-fold increase, and $V3_{I309pen-F317pen}$ exhibited approximately 6-fold decrease in the dissociation constant in comparison with the corresponding peptides containing cysteine at the same positions (Table 1). Thus, the use of penicillamine instead of cysteine did not exhibit any advantage and was slightly detrimental to 447-52D binding.

Replacement of L*-Proline with* D*-Proline or Asparagine*. The sequence D-Pro-Gly has been found to promote the formation of a β-hairpin (*48*, *49*). Similarly, Asn-Gly can stabilize β-hairpin structures (*50*). Hence, we wanted to examine whether D-Pro or Asn could substitute for L-Pro in the GPGR region of V3 peptides. SPR measurements revealed that V3 (L-Pro313D-Pro) exhibited more than a 50-fold increase in the dissociation constant relative to linear $V3_{CONSENSUS}$. The Pro313Asn replacement abolished completely the V3 peptide binding to 447-52D.

Dissociation Constant of Peptides Constrained by Double Disulfide Bonds. We synthesized six different V3 peptides constrained by double disulfide bonds in order to further constrain V3 to the postulated R5A, R5B, and X4 V3 conformations as listed in Table 2. SPR results obtained for these highly constrained molecules underline the reduction in affinity due to disulfide bonds involving the two residues flanking the GPGR, I309 and A316. It is interesting to compare the peptides constrained by a single disulfide bond close to the GPGR with peptides that contain an additional disulfide bond further away from the GPGR segment. While for the peptide $V3_{T303C-E322C;I309C-A316C}$ the dissociation constant decreased upon the introduction of a disulfide bond between residues 303 and 322 by 7-fold in comparison with $V3_{I309C-A316C}$, the dissociation constant of $V3_{R304C-G321C;H308C-F317C}$ increased by 14-fold in comparison to $V3_{H308C-F317C}$. The peptide $V3_{T303C-I323C;I307C-T319C}$, in which the disulfide bond was further removed from the GPGR segment, exhibited high affinity to 447-52D Fab that was only 4-fold lower than the affinity of the linear $V3_{CONSENSUS}$ peptide. Of the peptides constrained by two disulfide bonds, $V3_{T303C-E322C;I307C-Y318C}$ exhibited the tightest binding to 447-52D with a K_D of 0.78 nM, which is practically the same K_D observed for linear $V3_{CONSENSUS}$.

Thermodynamic Parameters of Linear versus Constrained Peptides. The thermodynamic values of linear and constrained V3 peptides were determined using isothermal titration calorimetry with the linear $V3_{CONSENSUS}$ peptide and the representative constrained peptide $V3_{T303C-E322C}$ (Figure 5). The ΔH value was determined from the ITC measurements. The $\Delta S°$ value was then calculated based on the free energy value ($\Delta G°$) from the K_a value obtained by SPR measurements (as described in Experimental Procedures). The linear $V3_{CONSENSUS}$ peptide exhibited a $\Delta H°$ value of −18.3 (±0.3) kcal/mol and a $\Delta S°$ of −20.0 (±0.3) cal/(mol·kelvin) while the constrained $V3_{T303C-E322C}$

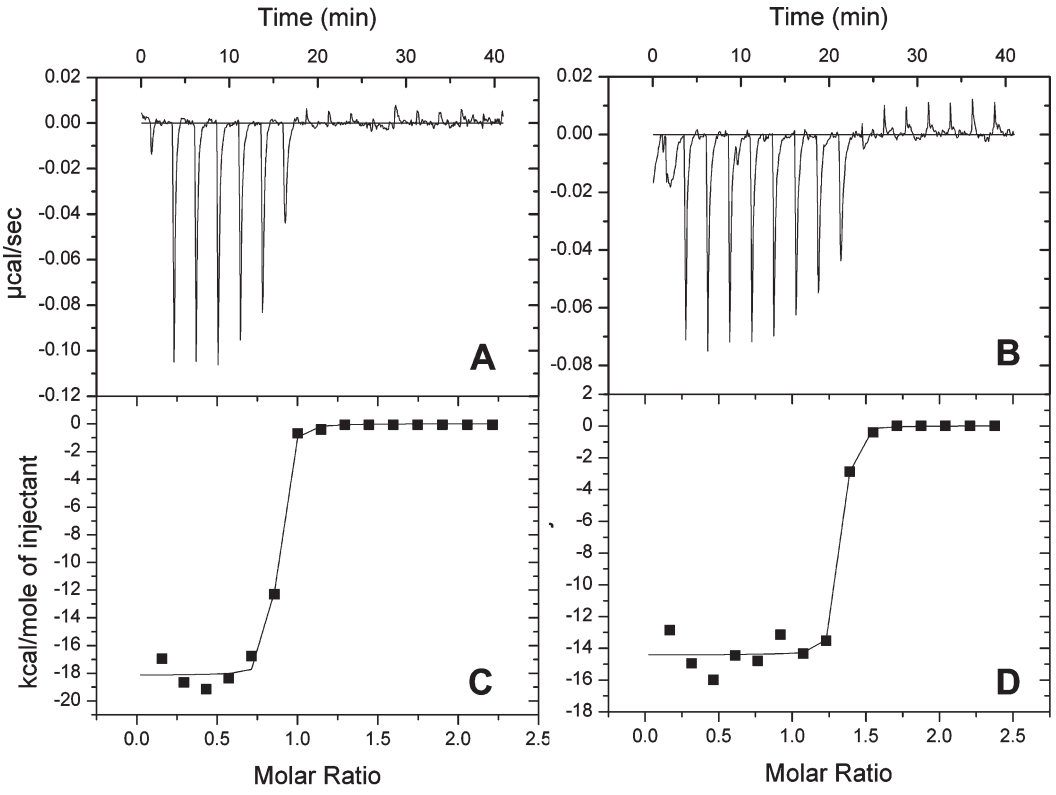

E	ΔH^0 kcal/mol	ΔS^0 cal/mol·kelvin
Linear	-18.3 (±0.3)	-20.0 (±0.3)
$V3_{T303C-E322C}$	-13.5 (±0.1)	-2.3 (±0.2)

FIGURE 5: Isothermal titration calorimetric (ITC) measurements of the binding of linear $V3_{CONSENSUS}$ and a representative constrained peptide to 447-52D Fab. Heat flow of linear $V3_{CONSENSUS}$ peptide (A) and constrained $V3_{T303C-E322C}$ peptide (B) added to 447-52D solution. Enthalpogram for linear $V3_{CONSENSUS}$ peptide (C) and constrained $V3_{T303C-E322C}$ peptide (D). Table summarizing the thermodynamic parameters (E).

exhibiteda $\Delta H°$ value of −13.5 (±0.1) kcal/mol and a $\Delta S°$ of −2.3 (±0.2) cal/(mol·kelvin). These results indicate different entropic and enthalpic contributions to the binding of linear and constrained peptides to 447-52D.

DISCUSSION

An important goal of our laboratory is to develop a rational approach to design an anti-V3 vaccine that will neutralize a broad spectrum of HIV-1 strains. To achieve this objective, we have designed and synthesized constrained V3 peptides that were expected to mimic the β-hairpin conformations recognized by 447-52D and to bind tightly to this broadly neutralizing anti-HIV-1 antibody. We assume that such constrained peptides can be used as immunogens to elicit an antibody response similar in potency and breadth of neutralization to 447-52D.

Constraining the peptide to a conformation similar to that recognized by the 447-52D antibody considerably reduced the change in the entropy of binding to the antibody in comparison with the entropy measured for the flexible linear $V3_{CONSENSUS}$ peptide binding (ΔS of −2.3 versus −20 cal/(mol·kelvin), respectively) as determined by ITC for $V3_{T303C-E322C}$ and linear $V3_{CONSENSUS}$. The enthalpic contribution to the free energy of binding was also smaller (in absolute value) for the constrained peptide in comparison with linear $V3_{CONSENSUS}$ (−13.5 vs −18.3 kcal/mol, respectively). The differences in the thermodynamic parameters observed for the binding of the free and linear $V3_{CONSENSUS}$ peptide reflect the preorganization of the constrained peptide and the formation of a hydrophobic cluster involving favorable energetic interactions between residues I307, I309, and F317 in the unbound constrained peptide (*43*). The more favorable entropy of binding of the constrained peptide to 447-52D is counterbalanced by a more favorable enthalpic contribution during binding of the linear $V3_{CONSENSUS}$ resulting in similar dissociation constants for both peptides.

Due to the use of disulfide bonds to constrain the V3 peptides, it is possible that some of the antibodies elicited by immunization with constrained V3 peptides will recognize the constraint itself and will, therefore, not cross-react with the V3 in its native context. The recognition of the constraint may depend on its location within the epitope recognized by the anti-V3 antibodies. Immunization with different constrained peptides and examination of the HIV-1 neutralizing potency of the immune sera are therefore required for the selection of the best vaccine candidate. Despite this concern, the results of the present study, together with our previous NMR investigation of constrained V3 peptides (*43*), clearly demonstrate that it is possible to constrain peptides to the

V3 β-hairpin-like conformation recognized by 447-52D while maintaining high-affinity binding to this HIV-1 neutralizing antibody.

A systematic change in the location of a disulfide bond within the V3 epitope recognized by the 447-52D antibody and determination of the binding of these constrained peptides to 447-52D have provided us with guidelines that will be used in the future to design the optimal constrained peptide immunogens for the induction of broadly neutralizing antibodies similar to 447-52D. A disulfide bond involving residues 309 and 316 or 309 and 317 reduced the affinity to 447-52D by 600- and 300-fold, respectively. Reduction of the disulfide bond in $V3_{I309C\text{-}F317C}$ caused a 100-fold decrease in K_D in comparison with the oxidized peptide. Moreover, mutation of I309 to alanine decreased the affinity to 447-52D only by 25-fold. Together, these results indicate that the disulfide bond connecting residues 309 and 316 or 309 and 317 must distort the cyclic peptide from the native V3 structure that binds to 447-52D, resulting in a major decrease in affinity to 447-52D.

Considerably higher affinity was obtained when T303, K305, or I307 was replaced by a cysteine residue and a disulfide bond between the N- and C-terminal strands was formed. The high-affinity binding of peptides constrained by disulfide bonds involving residues 303, 305, or 307 and the increased affinity of 447-52D Fab to oxidized vs reduced $V3_{T303C\text{-}E322C}$ peptides underline the gain in binding affinity, in comparison with the linear $V3_{CONSENSUS}$ peptide, achieved by constraining the peptides to a conformation similar to the V3 β-hairpin.

Replacement of I307 and T319 with cysteine resulted in a constrained peptide in which the segment C307−C319 mimicked a β-hairpin very well (*43*). However, the segments R304−S306 and T320−E322, which were part of the β-hairpin in $V3_{CONSENSUS}$ bound to 447-52D, were quite flexible in $V3_{I307C\text{-}T319C}$ as judged by our NMR analysis (*43*). Therefore, it is questionable whether this peptide would be an appropriate immunogen for eliciting 447-52D-like antibodies. The peptides constrained to the R5 conformations by a disulfide bond involving either T303 or K305 could be better vaccine candidates since in these two peptides either the entire V3 epitope or its major fraction is constrained while retaining high-affinity binding to 447-52D.

In our previous NMR studies (*43*) we have shown that disulfide bonds, especially in peptides constrained by two disulfide bonds, can dictate the pairing of the residues and the hydrogen bond network within the constrained peptide to mimic the postulated X4, R5A, and R5B conformations of the V3. Here we showed that V3 peptides constrained to the postulated X4 conformation exhibited poorer binding to 447-52D (Table 1 and Figure 4) and therefore are not appropriate candidates for anti-HIV-1 vaccine targeting R5 viruses. In contrast, peptides constrained to the R5A or the R5B conformations (*18*, *25*) of the V3 maintain high-affinity binding to 447-52D and as such are good candidates for an anti-HIV-1 vaccine that aims to target the R5 viruses which present the major challenge for HIV-1 vaccine development.

It should be noted that similar dissociation constants (K_D) were observed for peptides constrained to the R5A or R5B conformation given that the same N-terminal strand replacements to cysteine were used ($V3_{T303C\text{-}I323C}$ and $V3_{T303C\text{-}E322C}$, $V3_{K305C\text{-}G321C}$ and $V3_{K305C\text{-}T320C}$, and $V3_{I307C\text{-}T319C}$ and $V3_{I307C\text{-}Y318C}$). Previous NMR and crystallographic studies of V3 peptide complexes with 447-52D concluded that the N-terminal strand of the V3 and the GPGR turn form most of the interactions with 447-52D, while the C-terminal strand had only a few interactions with the antibody (*18*, *21*).

As for the peptides constrained by two disulfide bonds, four of the six V3 peptides investigated exhibited 2 orders of magnitude poorer affinity than the linear $V3_{CONSENSUS}$ parent peptide (Table 2). However, the $V3_{T303C\text{-}I323C;I307C\text{-}T319C}$ and $V3_{T303C\text{-}E322C;I307C\text{-}Y318C}$ peptides exhibited binding to 447-52D that was similar to that observed for the linear $V3_{CONSENSUS}$ peptide. The structure of these two peptides has not been determined. Nevertheless, the NMR structures of two other peptides constrained by two disulfide bonds indicate that such peptides form an almost ideal β-hairpin conformation when the two cysteine residues in each peptide analogue are separated by three residues (*43*). On the basis of the assumed structural mimicry and the high affinity of $V3_{T303C\text{-}I323C;I307C\text{-}T319C}$ and $V3_{T303C\text{-}E322C;I307C\text{-}Y318C}$ to 447-52D, these two peptides are excellent candidates for an HIV-1 vaccine component that targets the V3. We are currently initiating efforts to synthesize such doubly constrained peptides in a form suitable for immunization.

Turn stabilizing replacements such as L-Pro313D-Pro and Pro313Asn either abolished or considerably reduced the affinity to 447-52D. This is not surprising since P313 of a $V3_{MN}$ peptide was found to interact extensively with 447-52D and occupies the center of the antibody binding site (*21*). Our results are in agreement with a previous study that found that the proline in the GPGR segment was invariant in 55 447-52D-binding peptides selected from a phage-display library (*51*). On the basis of the proline replacements and the systematic change of the single disulfide bond, we conclude that in order to maintain optimal binding to 447-52D no modification should be conducted at the center of the V3 447-52D epitope which includes residues ^{308}HIGPGRAF^{317}.

Interestingly most of the V3 peptides used in this study exhibited on-rates in a very narrow range (0.2−0.7 10^6 s^{-1} M^{-1}, Table 1) regardless of whether they were linear or constrained by disulfide bonds. The existence of a significant population in a β-turn conformation formed by the GPGR segment even in the linear $V3_{CONSENSUS}$ peptide (*36*, *37*) and the dominant interaction of this segment with the center of anti-V3 antibodies (*21*) may contribute to the fast on-rate of the linear $V3_{CONSENSUS}$ peptide. It is possible that higher on-rates could not be determined accurately due to the limitation of the SPR method; thus, the SPR method has its limitations in distinguishing between peptides exhibiting very tight binding and high on-rates.

Despite the fact that we could mimic the native conformation of the V3 and retain high-affinity binding, the presentation of the V3 in the context of the entire gp120 may also be important in eliciting broadly neutralizing antibodies. Mimicking the presentation of V3 in the context of the entire gp120 is hard to achieve using short constrained peptides.

In conclusion, we have shown that structural information obtained by NMR studies of the V3 epitope recognized by anti-HIV-1 broadly neutralizing antibodies (*18*, *25*) can be used to design constrained V3 peptides in which the β-hairpin conformation of the antibody-bound V3 is stabilized to various degrees (*43*) while maintaining high-affinity binding to the antibody. Previous studies by Haynes and co-workers have shown that immunization with linear V3 peptides that contained the entire epitope recognized by the 447-52D antibody elicited a broadly neutralizing antibody response (*29*). It remains to be seen whether the additional

stabilization of the V3 peptide β-hairpin conformation will result in better vaccine candidates in comparison with linear V3 peptides.

ACKNOWLEDGMENT

We thank Dr. Zolla-Pazner for the 447-52D cell line, Dr. Gideon Schreiber and his students, especially Mr. Ori Cohavi, for letting us use the ProteOn instrument and for advice on the binding experiments, Dr. Irina Shin from the Biological Services for ITC experiments, and Mr. Yehezkiel Hayek for excellent technical assistance in peptide purification.

REFERENCES

1. Rusche, J. R., Javaherian, K., McDanal, C., Petro, J., Lynn, D. L., Grimaila, R., Langlois, A., Gallo, R. C., Arthur, L. O., and Fischinger, P. J.; et al. (1988) Antibodies that inhibit fusion of human immunodeficiency virus-infected cells bind a 24-amino acid sequence of the viral envelope, gp120. *Proc. Natl. Acad. Sci. U.S.A. 85*, 3198–3202.
2. Rosen, O., Chill, J., Sharon, M., Kessler, N., Mester, B., Zolla-Pazner, S., and Anglister, J. (2005) Induced fit in HIV-neutralizing antibody complexes: evidence for alternative conformations of the gp120 V3 loop and the molecular basis for broad neutralization. *Biochemistry 44*, 7250–7258.
3. Wu, L., Gerard, N. P., Wyatt, R., Choe, H., Parolin, C., Ruffing, N., Borsetti, A., Cardoso, A. A., Desjardin, E., Newman, W., Gerard, C., and Sodroski, J. (1996) CD4-induced interaction of primary HIV-1 gp120 glycoproteins with the chemokine receptor CCR-5. *Nature 384*, 179–183.
4. Trkola, A., Dragic, T., Arthos, J., Binley, J. M., Olson, W. C., Allaway, G. P., Cheng Mayer, C., Robinson, J., Maddon, P. J., and Moore, J. P. (1996) CD4-dependent, antibody-sensitive interactions between HIV-1 and its co-receptor CCR-5. *Nature 384*, 184–187.
5. Gorny, M. K., Conley, A. J., Karwowska, S., Buchbinder, A., Xu, J. Y., Emini, E. A., Koenig, S., and Zolla-Pazner, S. (1992) Neutralization of diverse human immunodeficiency virus type 1 variants by an anti-V3 human monoclonal antibody. *J. Virol. 66*, 7538–7542.
6. Gorny, M. K., Xu, J. Y., Karwowska, S., Buchbinder, A., and Zolla-Pazner, S. (1993) Repertoire of neutralizing human monoclonal antibodies specific for the V3 domain of HIV-1 gp120. *J. Immunol. 150*, 635–643.
7. Binley, J. M., Wrin, T., Korber, B., Zwick, M. B., Wang, M., Chappey, C., Stiegler, G., Kunert, R., Zolla-Pazner, S., Katinger, H., Petropoulos, C. J., and Burton, D. R. (2004) Comprehensive cross-clade neutralization analysis of a panel of anti-human immunodeficiency virus type 1 monoclonal antibodies. *J. Virol. 78*, 13232–13252.
8. Keele, B. F., Giorgi, E. E., Salazar-Gonzalez, J. F., Decker, J. M., Pham, K. T., Salazar, M. G., Sun, C., Grayson, T., Wang, S., Li, H., Wei, X., Jiang, C., Kirchherr, J. L., Gao, F., Anderson, J. A., Ping, L. H., Swanstrom, R., Tomaras, G. D., Blattner, W. A., Goepfert, P. A., Kilby, J. M., Saag, M. S., Delwart, E. L., Busch, M. P., Cohen, M. S., Montefiori, D. C., Haynes, B. F., Gaschen, B., Athreya, G. S., Lee, H. Y., Wood, N., Seoighe, C., Perelson, A. S., Bhattacharya, T., Korber, B. T., Hahn, B. H., and Shaw, G. M. (2008) Identification and characterization of transmitted and early founder virus envelopes in primary HIV-1 infection. *Proc. Natl. Acad. Sci. U.S.A. 105*, 7552–7557.
9. Wu, X., Sambor, A., Nason, M. C., Yang, Z. Y., Wu, L., Zolla-Pazner, S., Nabel, G. J., and Mascola, J. R. (2008) Soluble CD4 broadens neutralization of V3-directed monoclonal antibodies and guinea pig vaccine sera against HIV-1 subtype B and C reference viruses. *Virology 380*, 285–295.
10. Madani, N., Schon, A., Princiotto, A. M., Lalonde, J. M., Courter, J. R., Soeta, T., Ng, D., Wang, L., Brower, E. T., Xiang, S. H., Do Kwon, Y., Huang, C. C., Wyatt, R., Kwong, P. D., Freire, E., Smith, A. B.III, and Sodroski, J. (2008) Small-molecule CD4 mimics interact with a highly conserved pocket on HIV-1 gp120. *Structure 16*, 1689–1701.
11. Van Herrewege, Y., Morellato, L., Descours, A., Aerts, L., Michiels, J., Heyndrickx, L., Martin, L., and Vanham, G. (2008) CD4 mimetic miniproteins: potent anti-HIV compounds with promising activity as microbicides. *J. Antimicrob. Chemother. 61*, 818–826.
12. Kwong, P. D., Doyle, M. L., Casper, D. J., Cicala, C., Leavitt, S. A., Majeed, S., Steenbeke, T. D., Venturi, M., Chaiken, I., Fung, M., Katinger, H., Parren, P. W., Robinson, J., Van Ryk, D., Wang, L., Burton, D. R., Freire, E., Wyatt, R., Sodroski, J., Hendrickson, W. A., and Arthos, J. (2002) HIV-1 evades antibody-mediated neutralization through conformational masking of receptor-binding sites. *Nature 420*, 678–682.
13. Overbaugh, J., and Rudensey, L. M. (1992) Alterations in potential sites for glycosylation predominate during evolution of the simian immunodeficiency virus envelope gene in macaques. *J. Virol. 66*, 5937–5948.
14. Shan, M., Klasse, P. J., Banerjee, K., Dey, A. K., Iyer, S. P., Dionisio, R., Charles, D., Campbell-Gardener, L., Olson, W. C., Sanders, R. W., and Moore, J. P. (2007) HIV-1 gp120 mannoses induce immunosuppressive responses from dendritic cells. *PLoS Pathog. 3*, e169.
15. Wyatt, R., Kwong, P. D., Desjardins, E., Sweet, R. W., Robinson, J., Hendrickson, W. A., and Sodroski, J. G. (1998) The antigenic structure of the HIV gp120 envelope glycoprotein. *Nature 393*, 705–711.
16. Chen, B., Vogan, E. M., Gong, H., Skehel, J. J., Wiley, D. C., and Harrison, S. C. (2005) Structure of an unliganded simian immunodeficiency virus gp120 core. *Nature 433*, 834–841.
17. Sharon, M., Rosen, O., and Anglister, J. (2005) NMR studies of V3 peptide complexes with antibodies suggest a mechanism for HIV-1 coreceptor selectivity. *Curr. Opin. Drug Discov. Dev. 8*, 601–612.
18. Sharon, M., Kessler, N., Levy, R., Zolla-Pazner, S., Gorlach, M., and Anglister, J. (2003) Alternative conformations of HIV-1 V3 loops mimic beta hairpins in chemokines, suggesting a mechanism for coreceptor selectivity. *Structure 11*, 225–236.
19. Tugarinov, V., Zvi, A., Levy, R., and Anglister, J. (1999) A cis proline turn linking two beta-hairpin strands in the solution structure of an antibody-bound HIV-1IIIB V3 peptide. *Nat. Struct. Biol. 6*, 331–335.
20. Tugarinov, V., Zvi, A., Levy, R., Hayek, Y., Matsushita, S., and Anglister, J. (2000) NMR structure of an anti-gp120 antibody complex with a V3 peptide reveals a surface important for co-receptor binding. *Struct. Folding Des. 8*, 385–395.
21. Stanfield, R. L., Gorny, M. K., Williams, C., Zolla-Pazner, S., and Wilson, I. A. (2004) Structural rationale for the broad neutralization of HIV-1 by human monoclonal antibody 447-52D. *Structure 12*, 193–204.
22. Stanfield, R. L., Gorny, M. K., Zolla-Pazner, S., and Wilson, I. A. (2006) Crystal structures of human immunodeficiency virus type 1 (HIV-1) neutralizing antibody 2219 in complex with three different V3 peptides reveal a new binding mode for HIV-1 cross-reactivity. *J. Virol. 80*, 6093–6105.
23. Bell, C. H., Pantophlet, R., Schiefner, A., Cavacini, L. A., Stanfield, R. L., Burton, D. R., and Wilson, I. A. (2008) Structure of antibody F425-B4e8 in complex with a V3 peptide reveals a new binding mode for HIV-1 neutralization. *J. Mol. Biol. 375*, 969–978.
24. Huang, C. C., Lam, S. N., Acharya, P., Tang, M., Xiang, S. H., Hussan, S. S., Stanfield, R. L., Robinson, J., Sodroski, J., Wilson, I. A., Wyatt, R., Bewley, C. A., and Kwong, P. D. (2007) Structures of the CCR5 N terminus and of a tyrosine-sulfated antibody with HIV-1 gp120 and CD4. *Science 317*, 1930–1934.
25. Rosen, O., Sharon, M., Quadt-Akabayov, S. R., and Anglister, J. (2006) Molecular switch for alternative conformations of the HIV-1 V3 region: implications for phenotype conversion. *Proc. Natl. Acad. Sci. U.S.A. 103*, 13950–13955.
26. Rini, J. M., Stanfield, R. L., Stura, E. A., Salinas, P. A., Profy, A. T., and Wilson, I. A. (1993) Crystal structure of a human immunodeficiency virus type 1 neutralizing antibody, 50.1, in complex with its V3 loop peptide antigen. *Proc. Natl. Acad. Sci. U.S.A. 90*, 6325–6329.
27. Ghiara, J. B., Stura, E. A., Stanfield, R. L., Profy, A. T., and Wilson, I. A. (1994) Crystal structure of the principal neutralization site of HIV-1. *Science 264*, 82–85.
28. Stanfield, R. L., Ghiara, J. B., Ollmann Saphire, E., Profy, A. T., and Wilson, I. A. (2003) Recurring conformation of the human immunodeficiency virus type 1 gp120 V3 loop. *Virology 315*, 159–173.
29. Haynes, B. F., Ma, B., Montefiori, D. C., Wrin, T., Petropoulos, C. J., Sutherland, L. L., Scearce, R. M., Denton, C., Xia, S. M., Korber, B. T., and Liao, H. X. (2006) Analysis of HIV-1 subtype B third variable region peptide motifs for induction of neutralizing antibodies against HIV-1 primary isolates. *Virology 345*, 44–55.
30. Liao, H. X., Etemad-Moghadam, B., Montefiori, D. C., Sun, Y., Sodroski, J., Scearce, R. M., Doms, R. W., Thomasch, J. R., Robinson, S., Letvin, N. L., and Haynes, B. F. (2000) Induction of antibodies in guinea pigs and rhesus monkeys against the human immunodeficiency virus type 1 envelope: neutralization of nonpathogenic and pathogenic primary isolate simian/human immunodeficiency virus strains. *J. Virol. 74*, 254–263.
31. Letvin, N. L., Robinson, S., Rohne, D., Axthelm, M. K., Fanton, J. W., Bilska, M., Palker, T. J., Liao, H. X., Haynes, B. F., and Montefiori, D. C. (2001) Vaccine-elicited V3 loop-specific antibodies

in rhesus monkeys and control of a simian-human immunodeficiency virus expressing a primary patient human immunodeficiency virus type 1 isolate envelope. *J. Virol. 75*, 4165–4175.
32. Someya, K., Cecilia, D., Ami, Y., Nakasone, T., Matsuo, K., Burda, S., Yamamoto, H., Yoshino, N., Kaizu, M., Ando, S., Okuda, K., Zolla-Pazner, S., Yamazaki, S., Yamamoto, N., and Honda, M. (2005) Vaccination of rhesus macaques with recombinant *Mycobacterium bovis bacillus* Calmette-Guerin Env V3 elicits neutralizing antibody-mediated protection against simian-human immunodeficiency virus with a homologous but not a heterologous V3 motif. *J. Virol. 79*, 1452–1462.
33. Hewer, R., and Meyer, D. (2005) Evaluation of a synthetic vaccine construct as antigen for the detection of HIV-induced humoral responses. *Vaccine 23*, 2164–2167.
34. Golding, B., Eller, N., Levy, L., Beining, P., Inman, J., Matthews, N., Scott, D. E., and Golding, H. (2002) Mucosal immunity in mice immunized with HIV-1 peptide conjugated to Brucella abortus. *Vaccine 20*, 1445–1450.
35. Liao, H. X., Haynes, B., Korber, B., De-Lorimier, R. M. (2004) Polyvalent Immunogen, W/O 2004/075850.
36. Chandrasekhar, K., Profy, A. T., and Dyson, H. J. (1991) Solution conformational preferences of immunogenic peptides derived from the principal neutralizing determinant of the HIV-1 envelope glycoprotein gp120. *Biochemistry 30*, 9187–9194.
37. Zvi, A., Hiller, R., and Anglister, J. (1992) Solution conformation of a peptide corresponding to the principal neutralizing determinant of HIV-1IIIB: a two-dimensional NMR study. *Biochemistry 31*, 6972–6979.
38. Santiveri, C. M., Leon, E., Rico, M., and Jimenez, M. A. (2008) Context-dependence of the contribution of disulfide bonds to beta-hairpin stability. *Chemistry 14*, 488–499.
39. Cabezas, E., Wang, M., Parren, P. W., Stanfield, R. L., and Satterthwait, A. C. (2000) A structure-based approach to a synthetic vaccine for HIV-1. *Biochemistry 39*, 14377–14391.
40. Cabezas, E., and Satterthwait, A. C. (1999) The hydrogen bond mimic approach: Solid-phase synthesis of a peptide stabilized as an alpha-helix with a hydrazone link. *J. Am. Chem. Soc. 121*, 3862–3875.
41. Conley, A. J., Conard, P., Bondy, S., Dolan, C. A., Hannah, J., Leanza, W. J., Marburg, S., Rivetna, M., Rusiecki, V. K., and Sugg, E. E.; et al. (1994) Immunogenicity of synthetic HIV-1 gp120 V3-loop peptide-conjugate immunogens. *Vaccine 12*, 445–451.
42. Chakraborty, K., Durani, V., Miranda, E. R., Citron, M., Liang, X., Schleif, W., Joyce, J. G., and Varadarajan, R. (2006) Design of immunogens that present the crown of the HIV-1 V3 loop in a conformation competent to generate 447-52D-like antibodies. *Biochem. J. 399*, 483–491.
43. Mor, A., Segal, E., Mester, B., Arshava, B., Rosen, O., Ding, F. X., Russo, J., Dafni, A., Schvartzman, F., Scherf, T., Naider, F., and Anglister, J. (2009) Mimicking the structure of the V3 epitope bound to HIV-1 neutralizing antibodies. *Biochemistry 48*, 3288–3303.
44. Sharon, M., Gorlach, M., Levy, R., Hayek, Y., and Anglister, J. (2002) Expression, purification, and isotope labeling of a gp120 V3 peptide and production of a Fab from a HIV-1 neutralizing antibody for NMR studies. *Protein Expression Purif. 24*, 374–383.
45. Bravman, T., Bronner, V., Lavie, K., Notcovich, A., Papalia, G. A., and Myszka, D. G. (2006) Exploring "one-shot" kinetics and small molecule analysis using the ProteOn XPR36 array biosensor. *Anal. Biochem. 358*, 281–288.
46. Myszka, D. G. (1999) Improving biosensor analysis. *J. Mol. Recognit. 12*, 279–284.
47. Leavitt, S., and Freire, E. (2001) Direct measurement of protein binding energetics by isothermal titration calorimetry. *Curr. Opin. Struct. Biol. 11*, 560–566.
48. Awasthi, S. K., Raghothama, S., and Balaram, P. (1995) A designed beta-hairpin peptide. *Biochem. Biophys. Res. Commun. 216*, 375–381.
49. Haque, T. S., Little, J. C., and Gellman, S. H. (1996) Stereochemical requirements for beta-hairpin formation: model studies with four-residue peptides and depsipeptides. *J. Am. Chem. Soc. 118*, 6975–6985.
50. Ramirez-Alvarado, M., Blanco, F. J., and Serrano, L. (1996) De novo design and structural analysis of a model beta-hairpin peptide system. *Nat. Struct. Biol. 3*, 604–612.
51. Keller, P. M., Arnold, B. A., Shaw, A. R., Tolman, R. L., Van Middlesworth, F., Bondy, S., Rusiecki, V. K., Koenig, S., Zolla-Pazner, S., and Conard, P.; et al. (1993) Identification of HIV vaccine candidate peptides by screening random phage epitope libraries. *Virology 193*, 709–716.